

1 **Identification of the Final Two Genes Functioning in Methanofuran Biosynthesis in**

2 *Methanocaldococcus jannaschii*

3

4 Yu Wang, Huimin Xu, Michael K. Jones, and Robert H. White*

5

6 *Department of Biochemistry, Virginia Polytechnic Institute and State University, Blacksburg,*

7 *Virginia 24061*

8

9

10 This work was supported by National Science Foundation Grant MCB1120346.

11

12 *To whom correspondence should be addressed. Telephone: (540) 231-6605, Fax: (540) 231-

13 9070, e-mail: rhwhite@vt.edu

14

15 **Running title:** methanofuran biosynthesis

16

17 **Keywords:** methanogenic cofactors.

18

ABSTRACT

All methanofuran structural variants contain a basic core structure of 4-[*N*-(γ -L-glutamyl)-*p*-(β -aminoethyl)phenoxyethyl]-(aminomethyl)furan (APMF-Glu), but have different side chains depending on the source organism. Recently, we identified four genes (MfnA, MfnB, MfnC, and MfnD) that are responsible for the biosynthesis of the methanofuran precursors γ -glutamyltyramine and 5-(aminomethyl)-3-furanmethanol-phosphate (F1-P) from tyrosine, glutamate, glyceraldehyde-3-P, and alanine in *Methanocaldococcus jannaschii*. How γ -glutamyltyramine and F1-P couple together to form the core structure of methanofuran was previously unknown. Here, we report the identification of two enzymes encoded by the genes *mj0458* and *mj0840* that catalyze the formation of F1-PP from ATP and F1-P and the condensation of F1-PP with γ -glutamyltyramine, respectively, to form APMF-Glu. We have annotated these enzymes as MfnE and MfnF, respectively, representing the fifth and sixth enzymes in the methanofuran biosynthetic pathway to be identified. Although MfnE was previously reported as an archaeal adenylate kinase, our present results show that MfnE is a promiscuous enzyme and its possible physiological role is to produce F1-PP. Unlike other enzymes catalyzing coupling reactions involving pyrophosphate as the leaving group, MfnF exhibits a distinctive α/β two-layer sandwich structure. By comparing MfnF with thiamine synthase and dihydropteroate synthase, an S_N1 reaction mechanism is proposed for MfnF. With the identification of MfnE and MfnF, the biosynthetic pathway for the methanofuran core structure APMF-Glu is complete.

42 **IMPORTANCE**

43 This work describes the identification of the final two enzymes responsible for catalyzing the
44 biosynthesis of the core structure of methanofuran. The gene products of *mj0458* and *mj0840*
45 catalyze the formation of F1-PP and the coupling of F1-PP with γ -glutamyltyramine,
46 respectively, to form APMF-Glu. Although the chemistry of such a coupling reaction is
47 widespread in biochemistry, this work provides the first evidence that such a mechanism is
48 employed in methanofuran biosynthesis. MfnF belongs to the hydantoinase-A family (PF01968)
49 and exhibits a unique α/β two-layer sandwich structure different from the enzymes catalyzing
50 similar reactions. Our results show that MfnF catalyzes the formation of an ether bond during
51 methanofuran biosynthesis. Therefore, this work further expands the functionality of this enzyme
52 family.

53

54

55

56

57

58

59

60

61

62 **M**ethanofuran is the first in a series of coenzymes involved in the biochemical reduction of
63 carbon dioxide to methane (1-3). This process, known as methanogenesis, is carried out only by
64 the methanogenic archaea, which produce more than 400 million tons of methane each year as an
65 essential part of the global carbon cycle (4). Methanofuran is the initial C1 acceptor molecule
66 involved in the first two-electron reduction of carbon dioxide to produce the formamide
67 derivative of methanofuran, where the formate is attached to the amino group of methanofuran
68 through methanogenesis (5). This is one of the few known pathways for carbon dioxide fixation
69 in Nature. In addition, methylotrophic bacteria also use methanofuran as a coenzyme to oxidize
70 formaldehyde to formic acid (6, 7). The chemical structure of methanofuran varies among
71 different methanogens (8); each currently known methanofuran molecule contains the basic core
72 structure of 4-[N-(γ -L-glutamyl)-p-(β -aminoethyl)phenoxy-methyl]-2-(amino-methyl)furan
73 (APMF-Glu), but isolated analogs have different attached side chains (8). Recently, our
74 laboratory identified a new methanofuran structure in *Methanocaldococcus jannaschii*, which
75 contains a long γ -glutamyl tail with 7-12 γ -linked glutamates (9) (Fig 1). Although the function
76 of methanofuran has been known for many years, its biosynthetic pathway has not been fully
77 elucidated.

78 Recently, we discovered the route for the production of 4-(hydroxymethyl)-2-
79 furancarboxaldehyde-P (4-HFC-P) from glyceraldehyde-3-P (10). The resulting 4-HFC-P
80 undergoes a transamination reaction to produce 5-(aminomethyl)-3-furanmethanol-phosphate
81 (F1-P) (10, 11), a precursor of the furan moiety of methanofuran (Fig 1). We previously
82 demonstrated that the *mj0050* gene encodes a tyrosine decarboxylase that produces tyramine
83 from tyrosine (12). A tyramine-glutamate ligase (the gene product of *mj0815*) catalyzes the ATP-
84 dependent addition of one glutamate to tyramine via a γ -linked amide bond (13) (Fig 1). To

85 produce APMF-Glu, we propose that one enzyme is required to catalyze the conversion of F1-P
86 to F1-PP, where the pyrophosphate group serves as a better leaving group in the subsequent
87 condensation reaction. Another enzyme then catalyzes the condensation between F1-PP and γ -
88 glutamyltyramine.

89 The homologs of *mj0458* and *mj0840* are widely distributed among the methanofuran-
90 containing organisms, including all methanogenic archaea and some methylotrophic bacteria.
91 Comparative genomic analysis shows that in some methanogens and methylotrophs, the
92 homologs of the *mj0458* and *mj0840* genes appear in the neighborhood of *mj0815* (Fig 2), which
93 encodes the enzyme that catalyzes the ATP-dependent addition of one glutamate to tyramine,
94 producing γ -glutamyltyramine. Therefore, the gene products of *mj0458* (MJ0458) and *mj0840*
95 (MJ0840) are likely to be involved in methanofuran biosynthesis. We reported that *mj0458*
96 encodes a second type of archaeal adenylate kinase that catalyzes phosphoryl group transfer from
97 one molecule of ATP to one molecule of AMP, generating two molecules of ADP (14). A similar
98 phosphoryl transfer reaction is expected to generate F1-PP from F1-P and ATP. It is possible that
99 the gene product of *mj0458* is a promiscuous enzyme, catalyzing both reactions. The gene
100 product of *mj0840* is an uncharacterized protein. PSI-blast analysis shows that it belongs to the
101 hydantoinase A family (PF01968) and contains a sugar kinase domain. However, the four
102 histidines (15) that are found in hydantoinase, which are catalytically essential, are not conserved
103 in the proteins encoded by *mj0840* and its homologues, indicating that the gene product of
104 *mj0840* is unlikely to function as a hydantoinase.

105 To test whether the gene products of *mj0458* and *mj0840* are involved in methanofuran
106 biosynthesis, we cloned and heterologously expressed both genes in *Escherichia coli*. Here, we
107 report that the purified protein expressed from the *M. jannaschii* gene locus *mj0458* catalyzes the

108 ATP-dependent phosphoryl transfer reaction to generate F1-PP from F1-P. The purified protein
109 expressed from the *M. jannaschii* gene locus *mj0840* catalyzes the condensation reaction
110 between F1-PP and γ -glutamyltyramine, likely via a S_N-1 reaction mechanism. These are the
111 fifth and sixth enzymes that we have identified in the methanofuran biosynthetic pathway;
112 therefore, we have annotated the gene products of *mj0458* and *mj0840* as MfnE and MfnF,
113 respectively.

114

115 MATERIALS AND METHODS

116 **Chemicals.** All reagents were purchased from Sigma-Aldrich unless otherwise specified.

117 **Chemical Synthesis of F1-P from 4-HFC-P.** The chemical synthesis of F1-P started from 4-
118 HFC-P, whose synthesis has been previously described (11), with the following changes. To
119 synthesize 4-HFC-P, 4-HFC (68 mg, 0.53 mmol) was dissolved in 2 mL of acetonitrile to which
120 was added 120 μ l of trichloroacetonitrile (1.2 mmol) and tetrabutylammonium phosphate (300
121 mg, 0.88 mmole). This procedure was patterned after a previously described method (16). After
122 four hours (at room temperature), solvent was evaporated with a stream of nitrogen gas and the
123 sample mixed with 2 mL of water and cooled overnight at 3°C. The resulting trichloroacetamide
124 crystals were separated by filtration and the resulting solution was passed through a Dowex 50
125 NH₄⁺ column (0.5 \times 2 cm) to remove the tetrabutylammonium cation. Portions of the resulting
126 solution were purified by preparative thin layer chromatography (TLC) as described before (11).
127 The reaction mixture containing 4-HFC-P was then evaporated to dryness and dissolved in 3 mL
128 of concentrated NH₄OH to which 11 mg of NaBH₄ was dissolved. At first, the sample was clear,
129 but after a few minutes it became cloudy. After 2 hours at room temperature the solution became
130 clear again and there was no borohydride present, as detected by a lack of hydrogen production

131 upon acidification of a small volume of the reaction mixture (2-3 μL). The reaction mixture was
132 then evaporated to remove ammonia and placed in 2 mL of water followed by pH adjustment to
133 < 4 using 1 M HCl. The resulting sample was then placed on a Dowex 50W8- H^+ column (0.8 x 4
134 cm) that was washed with 2 mL of 20 mM HCl. The F1-P was retained on the column under
135 these conditions. The elution of F1-P was begun by passing 2 mL water through the column and
136 completed with an additional elution using 3 M NH_4OH . Thin-layer chromatography (TLC)
137 analysis with ninhydrin detection of amines showed that the water fraction contained F1-P as the
138 only detectable compound. The F1-P was further purified by preparative TLC using the solvent
139 system (acetonitrile, water, and 88% formic acid (40:20:10 vol/vol/vol)) where it had an $R_f =$
140 0.21. The ammonia fraction contained most of the F1-P and also ammonium-containing salts that
141 was detected by the ninhydrin. The total yield of F1-P was 18%. Both F1 and F1-P showed an
142 absorbance maximum at 215 nm, similar to 2,5-dimethylfuran. The concentration of F1-P was
143 estimated based on the extinction coefficient of 2,5-dimethylfuran ($\epsilon_{215} = 7900 \text{ M}^{-1} \text{ cm}^{-1}$) (17).

144 **Analysis of F1 and its Derivatives.** Direct analysis of F1 by HPLC is difficult due to the
145 short wavelength at which F1 absorbs (215 nm), which is common to many compounds, and the
146 fact that F1 is not retained by reverse-phase HPLC columns. In this study, F1, F1-P, and F1-PP
147 were each converted to the 7-nitrobenzofurazan (NBD)-derivative, as previous reported (10).
148 NBD-F1-P was purified by preparative TLC using the solvent system (5% formic acid in
149 acetonitrile), where NBD-F1-P had an $R_f = 0.15$. After removal from the TLC plate, the structure
150 of the NBD-derivatives were then confirmed using HPLC (see below) and LC- electrospray
151 ionization-MS (LC-ESI-MS) analysis (10).

152 **HPLC Analysis of NBD-F1, NBD-F1-P, and NBD-F1-PP Derivatives.** Chromatographic
153 separation of NBD derivatives was performed on a Shimadzu HPLC System (UFLC) equipped

154 with a C18 reverse phase column (Kromasi 100-5-C₁₈, 4.6 × 250 mm). The elution profile
155 consisted of 5 min at 95% sodium acetate buffer (25 mM, pH 6.0, in presence of 0.02% NaN₃)
156 and 5% MeOH followed by a linear gradient to 45% sodium acetate buffer/55% MeOH over 35
157 min at 1.0 mL/min. F1-NBD derivatives were detected by fluorescence using an excitation
158 wavelength of 480 nm and an emission wavelength of 542 nm. Under these conditions, NBD
159 derivatives were eluted in the following order (min): NBD-F1-PP (14.5), NBD-F1-P (17.0), and
160 NBD-F1 (20.9).

161 **HPLC Analysis of ATP, ADP, and AMP.** The separation and analysis of ATP, ADP, and
162 AMP in the sample were measured using a gradient ion pairing method performed on a
163 Shimadzu UFLC System equipped with a C₁₈ reverse phase column (ODS 250 × 4.6 mm, 5 μm
164 particle size) and a photodiode array detector (PDA). The elution profile consisted of 5 min at
165 100% Buffer A (0.1 M KH₂PO₄, 10 mM [CH₃(CH₂)₃]₄N(Br), pH 3.0) and 0% methanol followed
166 by a linear gradient to 25% Buffer A/75% methanol over 20 min at 1.0 mL/min. ATP, ADP, and
167 AMP were detected by absorbance at 260 nm. Under these conditions, ATP eluted at 10.8 min,
168 ADP eluted at 5.7 min, and AMP eluted at 4.1 min.

169 **LC-MS Analysis of the 4-[N-(γ-L-glutamyl)-p-(β-aminoethyl)phenoxyethyl]-2-(amino-**
170 **methyl)furan (APMF-Glu).** Analysis was performed with an AB Sciex 3200 Q TRAP mass
171 spectrometer system with an Agilent 1200 Series liquid chromatograph. A Zorbax (100 × 4.0
172 mm, 2.6 μm particle size) column was used and the injection volume was 15 μL. Solvent A was
173 water with 25 mM ammonium acetate and solvent B was methanol. The flow rate was 0.5
174 mL/min. Gradient elution was employed in the following manner (t (min), %B): (0.01, 5), (10,
175 65), (15, 65), (15.01, 5). Column effluent was passed through a variable wavelength detector set
176 from 200 - 800 nm and then into the Turbo Spray ion source. Electrospray ionization (ESI) was

177 employed at -4500 volts and a temperature of 600 °C. Curtain gas, gas 1, and gas 2 flow
178 pressures were 35, 70, and 60 psi, respectively. Desolvation, entrance, and collision cell entrance
179 potentials were -40, -12, and -22.5 volts, respectively.

180 **Cloning of *M. jannaschii* *mj0458* and *mj0840* Genes and Expression of their Gene**

181 **Products.** The *mj0458* and *mj0840* genes were amplified from *M. jannaschii* genomic DNAs.

182 The primers used for *mj0458* were *mj0458*-Fwd: 5'-

183 GGTGGTCATATGCATATAGTAAAAATTGG-3' and *mj0458*-Rev: 5'-

184 GATCGGATCCTTATATTTTATCTATTCC-3'. The primers used for *mj0840* were *mj0840*-

185 Fwd: 5'-GTGTTTGATGTTAATGGGAATTTTAACTTCAGAAG-3' and *mj0840*-Rev: 5'-

186 CTTCTGAAGTTAAAAAATCCCATTAACATCAAACAC-3'. PCR amplifications were

187 performed at 55 °C as the annealing temperature. The PCR products were purified, digested with

188 *Nde*I and *Bam*HI restriction enzymes and then ligated into compatible sites in plasmid pT7-7 to

189 make the recombinant plasmid *pmj0458* and *pmj0840*. The sequences were verified by

190 sequencing at the University of Iowa DNA core facility. The resulting plasmids were used to

191 transform the *E. coli* BL21-Codon Plus (DE3)-RIL (Stratagene). Transformed cells were grown

192 in Lysogeny broth (LB)-medium (200 mL) supplemented with 100 µg/mL ampicillin at 37 °C

193 with shaking until an OD₆₀₀ of 1.0. Recombinant protein production was induced by addition of

194 lactose to a final concentration of 28 mM. After an additional 4 hours of culture at 37°C, the

195 cells were harvested by centrifugation (4000g, 5 min) and frozen at -20 °C. SDS-PAGE analysis

196 of total cellular proteins confirmed the induction of the gene products of *mj0458* and *mj0840* by

197 the appearance of intense protein bands at the expected 24 kDa and 37 kDa molecular weights,

198 respectively.

199 **Purification of the Gene Products of Recombinant *mj0458* and *mj0840*.** The frozen *E. coli*

200 cell pellet (~0.4 g wet weight from 200 mL of growth medium) was suspended in 3 mL of
201 extraction buffer (50 mM N-[tris(hydroxymethyl)methyl]2-aminoethanesulfonic acid (TES), 10
202 mM MgCl₂, 20 mM Dithiothreitol (DTT) at pH 7.0) and lysed by sonication. The crude lysate
203 was then treated by benzonase nuclease (250 U). The protein products from *mj0458* and *mj0840*
204 were found to remain soluble after heating to 80 °C. Therefore, purification of the gene products
205 of *mj0458* and *mj0840* started by heating the resulting cell extracts for 10 min at 80 °C followed
206 by centrifugation (16000g, 10 min). This process allowed purification of the desired enzymes
207 from the majority of *E. coli* proteins, which denature and precipitate under these conditions.
208 Supernatant of the gene product of *mj0458* was then pooled and dialyzed against buffer
209 containing 50 mM TES and 10 mM MgCl₂, at pH 7.0. Further purification of the gene product of
210 *mj0840* was performed by anion-exchange chromatography of the 80 °C soluble fractions on a
211 MonoQ HR column (1 × 8 cm; Amersham Bioscience) using a linear gradient from 0 to 1 M
212 NaCl in 25 mM Tris buffer (pH 7.5), over 82 min at a flow rate of 1 mL/min.

213 **Enzymatic Assay of MfnE (gene product of *mj0458*).** To test whether MfnE could catalyze
214 the formation of F1-PP from F1-P and ATP, 80 μM F1-P and 500 μM ATP in the presence of 3.7
215 μM MfnE was incubated at 70°C for 60 min in 50 mM TES buffer in the presence of 5 mM Mg²⁺
216 and 5 mM K⁺ at pH 7.0. The reaction mixture was then converted to the NBD-derivatives and
217 analyzed by HPLC as described above.

218 To measure the MfnE activity, the reaction was conducted in a 100 μL reaction volume
219 containing 1.9 μM of MfnE, 200 μM F1-P or AMP, and 500 μM ATP in 50 mM 4-
220 morpholineethanesulfonic acid (MES) buffer in the presence of 5 mM Mg²⁺ and 5 mM K⁺ at pH
221 7.0 for 20 min at 80 °C. Following incubation, the reactions were quenched by the addition of 10

222 μL 1 M HCl, the precipitated protein was removed by centrifugation (16000g, 10 min), and the
223 resulting sample was neutralized by adding 8.3 μL 1.5 M, pH 8.8, Tris buffer.

224 **Metal and pH-Dependence of the MfnE Catalyzed Reaction.** For the metal-dependent
225 study, the standard enzymatic assays were carried out including 5 mM of one of the following
226 cations: Mg^{2+} , Mn^{2+} , Ni^{2+} , Co^{2+} , Cu^{2+} , Zn^{2+} , K^{+} or 10 mM EDTA in the standard assay. To
227 investigate the influence of pH on catalytic ability, the specific activity at varying pH's was
228 measured. The standard enzymatic assay was conducted in 25 mM citrate buffer (pH 4.0 - 6.0),
229 25 mM MES buffer (pH 6.0 - 7.0), and 25 mM tricine/3-(cyclohexylamino)1-propanesulfonic
230 acid (CAPS)/TES buffer (pH 6.7 to 11.5).

231 **Standard Enzymatic Assay of MfnF (gene product of *mj0840*).** The standard assay for
232 measuring MfnF enzymatic activity was conducted at 50 °C for 40 min in a 120 μL reaction
233 volume containing 5.2 μg of MfnF (40 μL), 40 μL MfnE catalyzed reaction mixture (containing
234 ~ 100 μM F1-PP), and 40 μL MfnD reaction mixture (13) (containing ~ 1 mM γ -
235 glutamyltyramine and ~ 4 mM tyramine), in 50 mM TES buffer in the presence of 5 mM Mg^{2+}
236 and 5 mM K^{+} at pH 7.0. Following incubation, the reactions were quenched by the addition of 10
237 μL 1 M HCl, the precipitated protein was removed by centrifugation (16000g, 10 min), and the
238 resulting sample was neutralized by adding 8.3 μL 1.5 M, pH 8.8, Tris buffer. The samples were
239 analyzed by LC-ESI-MS in the positive ion mode.

240

241 RESULTS

242 **Synthesis and Analysis of F1-P Derivatives.** F1-P was chemically synthesized from 4-
243 HFC-P and converted into the NBD-derivative. HPLC with fluorescence detector analysis
244 showed that NBD-F1-P eluted as a single peak at 17.0 min (Fig 3). After treatment with 1 μL

245 phosphatase (0.2 U/L), NBD-F1-P was converted to NBD-F1 (20.9 min), which co-eluted with
246 NBD-F1 (10). LC-ESI-MS analysis of NBD-F1-P showed a single peak with $MH^+ = 371.4\ m/z$
247 and $(M - H)^- = 369.4\ m/z$. MS/MS of the $(M - H)^- = 369.4$ ion showed fragments at 79, 97, 179,
248 289, and 323 (Fig 4A).

249 **Recombinant Expression, Purification, and Analysis of the Gene Products of *mj0458* and**
250 ***mj0840*.** Two genes at the loci of *mj0458* and *mj0840* were cloned and overexpressed in *E. coli*.
251 Their gene products were purified as described above. The purified proteins migrated as single
252 bands and were greater than 90% pure with an apparent molecular mass of 24 kDa (gene product
253 of *mj0458*) and 37 kDa (gene product of *mj0840*) (Fig 5). The identities of the purified proteins
254 were also confirmed by matrix-assisted laser desorption/ionization (MALDI)-MS analysis of the
255 tryptic-digested protein band from the SDS gel based on a previously described procedure (18).

256 **The Promiscuity of the Gene Product of *mj0458* (MfnE).** We had reported that the gene
257 product of *mj0458* encodes an adenylate kinase that catalyzes the transfer of a phosphoryl group
258 from ATP to AMP, producing two molecules of ADP (14). In addition to the gene product of
259 *mj0458* (MfnE), it is known that another archaeal adenylate kinase in *M. jannaschii* is the
260 product of the *mj0479* gene (19, 20). However, it was unexpected that methanogens would
261 contain two distinct adenylate kinases. Incubation of the gene product of *mj0458* with F1-P in the
262 presence of ATP clearly showed the formation of F1-PP and ADP. A control experiment
263 containing the same concentration of substrates in the absence of MfnE showed none of the
264 expected product (data not shown). Generation of ADP from the MfnE reaction was detected by
265 ion pairing HPLC, and the formation of F1-PP was confirmed using HPLC and LC-ESI-MS after
266 conversion to NBD-F1-PP. The NBD-F1-PP was observed as a new HPLC peak eluting at 14.5
267 min with a corresponding decrease in the intensity of the NBD-F1-P (17.0 min) peak (Fig 3).

268 LC-ESI-MS analysis of the NBD-derivative of the MfnE reaction mixture showed a single peak
269 with $MH^+ = 451.5\ m/z$ and $(M - H)^- = 449.5\ m/z$. MS/MS of the $(M - H)^- = 449.5$ ion showed
270 fragments at 79, 159, 177, 385, 403, and 431 (Fig 4B), which are consistent with NBD-F1-PP's
271 molecular weight and structure. These results clearly showed MfnE to catalyze the phosphoryl-
272 transfer reaction between ATP and F1-P producing ADP and F1-PP.

273 The pH-dependent study of MfnE activity showed a pH optimum at 7.0. We also observed
274 that MfnE exclusively employed Mg^{2+} as a cofactor to facilitate phosphoryl group transfer.
275 Addition of 10 mM EDTA to the reaction mixture resulted in complete loss of MfnE activity.
276 The activity of MfnE at 80°C was 0.16 $\mu\text{mol}/\text{mg}/\text{min}$ using F1-P as substrate and 0.072
277 $\mu\text{mol}/\text{mg}/\text{min}$ when AMP was employed as substrate (both of these values are the extent of
278 substrate conversion to product for each incubation). The adenylate kinase activity of MfnE 80°C
279 is 500 fold less than that of the gene product of *mj0479*, which encodes the first archaeal
280 adenylate kinase identified in *M. jannaschii* (19). In addition, The homologs of *mj0458* in some
281 methanogens and methylotrophs cluster with MfnD (*mj0815*), which encodes the enzyme that
282 catalyzes γ -glutamyltyramine formation during methanofuran biosynthesis (13). These results
283 strongly suggest that the possible physiological function of MfnE is to catalyze the formation of
284 F1-PP involved in methanofuran biosynthesis.

285 **The Gene Product of *mj0840* (MfnF) Catalyzes the Formation of APMF-Glu.** The gene
286 product of *mj0840* was annotated as a hypothetical protein in *M. jannaschii* (21). Incubation of
287 the purified gene product of *mj0840* (MfnF) with γ -glutamyltyramine and F1-PP, which are
288 generated from the MfnE and MfnD catalyzed reactions, respectively, clearly showed the
289 formation of APMF-Glu. This was confirmed with mass spectral data showing a single peak
290 with the expected $(M - H)^- = 374.2\ m/z$ and $MH^+ = 376.2\ m/z$. The extracted ion chromatograph

(XIC) of the product with $MH^+ = 376.2$ m/z eluted as a single peak at 18 min (Fig 6A and 6B). The identity of APMF-Glu was also supported by MS/MS data (Fig 6C) with the $MH^+ = 376.2$ ion producing expected fragments at 110, 213, 230, and 267. Also, incubation of γ -glutamyltyramine plus F1-PP in the absence of MfnF showed that no APMF-Glu was formed under the same conditions (data not shown). When incubating γ -glutamyltyramine and F1-P in the presence of MfnF, a trace of APMF-Glu was observed in LC/MS (Fig 6A), but the intensity was less than 2% of that when F1-PP was used as substrate. In addition, MfnF could not use tyramine as a substrate to condense with F1-PP, since no APMF ($(M - H)^+ = 245.1$ m/z and $MH^+ = 247.1$ m/z) was detected from the mass spectral data, consistent with our previous hypothesis that condensation of the tyramine moiety with F1-PP must occur after formation of γ -glutamyltyramine (13).

DISCUSSION

Methanofuran is the initial C1 acceptor molecule in the formation of methane through methanogenesis. Several structurally different methanofurans are currently known, with the nature of the differences residing in modifications of the side chain attached to the basic core APMF-Glu structure found in all methanofurans (9). With the discovery of MfnA, MfnB, MfnC, and MfnD, the possible biosynthetic pathway of APMF-Glu was proposed (Fig 1). In this pathway, at least two enzymes are required to condense F1-P with γ -glutamyltyramine moiety. One enzyme is required to catalyze the conversion of F1-P to F1-PP, where the pyrophosphate group serves as a better leaving group for the subsequent condensation reaction. The other enzyme catalyzes the condensation between F1-PP and γ -glutamyltyramine to produce APMF-

313 Glu. Such a coupling mechanism is a common strategy used in the biosynthesis of coenzymes
314 such as folate (22) and thiamine (23) as well as terpenes and steroids (24-26).

315 During thiamine biosynthesis, ThiD (4-amino-5-hydroxymethyl-2-methylpyrimidine
316 phosphate (HMP-P) kinase) phosphorylates HMP-P to 4-amino-5-hydroxymethyl-2-
317 methylpyrimidine pyrophosphate (HMP-PP), and then another enzyme, thiamin phosphate
318 synthase (ThiE), catalyzes the coupling reaction of HMP-PP and 4-methyl-5-
319 hydroxyethylthiazole phosphate (23). During folate biosynthesis, the formation of 6-
320 hydroxymethyl-7,8-dihydropterin pyrophosphate (H₂HMP-PP) is catalyzed via a one-step
321 pyrophosphoryl-transfer reaction directly from 6-hydroxymethyl-7,8-dihydropterin, then
322 dihydropteroate synthase catalyzes the condensation of H₂HMP-PP and *p*-aminobenzoic acid
323 (22). Similarly, to condense the F1-P moiety and γ -glutamyltyramine in the methanofuran
324 biosynthesis pathway, a kinase is likely involved in transferring a phosphoryl group to form F1-
325 PP before the condensation step. This assumption is based on the fact that 1) the pyrophosphate
326 group serves as a better leaving group compared to a phosphate group because pyrophosphate is
327 a stronger acid compared to a phosphate group and 2) pyrophosphate complexes to magnesium
328 ions to form a ubiquitous leaving group.

329 We previously reported that MfnE encodes a second type of archaeal adenylate kinase (14). In
330 addition to MfnE, it has been established that another archaeal adenylate kinase in *M. jannaschii*
331 is the product of the *mj0479* gene (19, 20). It is unlikely that methanogens would contain two
332 distinct adenylate kinases. Our results clearly show that the promiscuous MfnE also catalyzes the
333 formation of F1-PP from F1-P and ATP. The gene locus *mj0458* is in the neighborhood of MfnD
334 (encoded by *mj0815*) and MfnF (encoded by *mj0840*), which are known to be involved in
335 methanofuran biosynthesis. We propose that the physiological function of MfnE is to catalyze

336 F1-PP formation during methanofuran biosynthesis. However, to approve our hypothesis, future
337 work will focus on screening the F1-PP kinase activity in other *M. jannaschii* kinases and further
338 characterization of MfnE.

339 Many promiscuous enzymes that have been found in archaea (27, 28). *M. jannaschii* is an
340 autotrophic archaea with a small genome (21). Therefore, promiscuity of enzymes can provide
341 an obvious advantage, allowing it to react with a broader range of substrates to maximize its
342 catalytic versatility using limited enzyme resources (29). Thus, the promiscuous MfnE may
343 possibly also perform a similar function to other adenylate kinases, which regulate the ATP/ADP
344 balance in the cell (14).

345 MfnF catalyzes the formation of an ether bond (C-O), instead of the C-N or C-C bond as
346 found in folate, thiamin, terpene, and steroid biosynthesis. The other well-known enzyme that
347 catalyzes C-O bond formation is geranylgeranyl glycerol phosphate synthase (GGGPS) (30). This
348 enzyme catalyzes the formation of an ether bond between glycerol-1-phosphate and polyprenyl
349 diphosphates, which is essential for biosynthesis of archaeal membrane lipid (30). GGGPS
350 exhibits an α/β TIM barrel structure (31), as does thiamine synthase (32) and dihydropteroate
351 synthase (33, 34).

352 PSI-blast analysis shows that MfnF belongs to the hydantoinase A family (PF01968) and
353 contains a sugar kinase domain. However, the catalytically essential histidines (15) in
354 hydantoinase are not conserved in MfnF. The crystal structure of the MfnF homolog in
355 *Methanococcus maripaludis*, which was solved by Kuzin, A. P. *et al.* (PDB: 3CET), exhibits a
356 distinctive α/β two-layer sandwich structure (Fig 7), unlike the α/β TIM barrel structure observed
357 in thiamine synthase (32), dihydropteroate synthase (33, 34) and GGGPS (31). In the active sites
358 of both the thiamine synthase and dihydropteroate synthase, the Mg^{2+} used to stabilize the

359 leaving pyrophosphate is found to be ligated by two aspartic acid residues (33, 35). Such a
360 pyrophosphate stabilizing interaction is similar to that found in farnesyl pyrophosphate synthase
361 (24), aristolochene synthase (25), and pentalenene synthase (26), which catalyze the formation of
362 an allylic carbocation from a pyrophosphate ester. In addition, serine and/or threonine residues
363 are hydrogen-bonded to the oxygen atom of the pyrophosphate to activate the pyrophosphate as a
364 leaving group (35). Sequence alignment and structural analysis of MfnF show a highly conserved
365 motif, D₁₃₅XGSTTXD₁₄₂, which is likely involved in metal and pyrophosphate binding during
366 catalysis. In addition, a strictly conserved Arg158 likely plays a role in stabilizing pyrophosphate
367 as a leaving group (Fig 7).

368 In all examples where pyrophosphate serves as a leaving group, it has been proposed that the
369 reaction mechanism follows an S_N-1 mechanism that proceeds via formation of a cationic
370 intermediate before nucleophilic attack by the other substrate (24-26, 33, 35). Therefore, it is
371 reasonable to assume that MfnF catalyzes a reaction following a similar mechanism (Fig 8). In
372 this mechanism, pyrophosphate is first removed from F1-PP, stabilized by the metal ion (likely
373 Mg²⁺) and Arg158 (Fig 7), where the resulting cationic intermediate species (F1⁺) is resonance
374 stabilized with the positive charge delocalized over the furan ring. The hydroxyl group of γ -
375 glutamyltyramine finally attacks F1⁺ at the C6 carbon atom to generate the product APMF-Glu.

376 In summary, this work describes two enzymes, MfnE and MfnF, that are responsible for the
377 formation of APMF-Glu with the first enzyme (MfnE) catalyzing the phosphorylation of F1-P to
378 F1-PP and the second enzyme (MfnF) catalyzing the coupling of F1-PP with γ -glutamyltyramine
379 to produce the core structure of methanofuran. Although such coupling reactions are ubiquitous
380 in biochemistry, this work provides the first evidence that such a mechanism is employed in
381 methanofuran biosynthesis. Since methanofuran in *M. jannaschii* contains 7-12 γ -linked

382 glutamates, we propose that once the core structure APMF-Glu is synthesized, another enzyme
383 catalyzes polyglutamylation, producing the final methanofuran molecule (Fig 1). However, we
384 have yet to identify the enzyme catalyzing this polyglutamylation.

385 **ACKNOWLEDGEMENTS**

386 The authors would like to thank Dr. Walter Niehaus for invaluable discussion and Dr. Janet
387 Webster for editing the manuscript. We also thank Dr. W. Keith Ray and Kim C. Harich for
388 performing the mass spectrometry experiments. The mass spectrometry resources are maintained
389 by the Virginia Tech Mass Spectrometry Incubator, a facility operated in part through funding by
390 the Fralin Life Science Institute at Virginia Tech and the Agricultural Experiment Station Hatch
391 Program (CRIS project no.: VA-135981).

392

393

394

395

396

397

398

399

400

401

402

403

404

405 REFERENCES

- 406 1. **Ferry JG.** 1999. Enzymology of one-carbon metabolism in methanogenic pathways.
407 FEMS Microbiol. Rev. **23**:13-38.
- 408 2. **Deppenmeier U.** 2002. The unique biochemistry of methanogenesis. Prog. Nucleic Acid
409 Res. Mol. Biol. **71**:223-283.
- 410 3. **Leigh JA, Rinehart KL, Wolfe RS.** 1984. Structure of Methanofuran, the Carbon-
411 Dioxide Reduction Factor of *Methanobacterium thermoautotrophicum*. *J. Am. Chem.*
412 *Soc.* **106**:3636-3640.
- 413 4. **Neue H.** 1993. Methane emissions from rice fields. BioScience **43**:466-476.
- 414 5. **Leigh JA, Rinehart KL, Jr., Wolfe RS.** 1985. Methanofuran (carbon dioxide reduction
415 factor), a formyl carrier in methane production from carbon dioxide in
416 *Methanobacterium*. Biochemistry **24**:995-999.
- 417 6. **Chistoserdova L, Vorholt JA, Thauer RK, Lidstrom ME.** 1998. C1 transfer enzymes
418 and coenzymes linking methylotrophic bacteria and methanogenic Archaea. Science
419 **281**:99-102.
- 420 7. **Pomper BK, Vorholt JA.** 2001. Characterization of the formyltransferase from
421 *Methylobacterium extorquens* AM1. Eur. J. Biochem. **268**:4769-4775.
- 422 8. **White RH.** 1988. Structural Diversity among Methanofurans from Different
423 Methanogenic Bacteria. J. Bacteriol. **170**:4594-4597.
- 424 9. **Allen KD, White RH.** 2014. Identification of structurally diverse methanofuran
425 coenzymes in methanococcales that are both *N*-formylated and *N*-acetylated.
426 Biochemistry **53**:6199-6210.

- 427 10. **Miller D, Wang Y, Xu H, Harich K, White RH.** 2014. Biosynthesis of the 5-
428 (Aminomethyl)-3-furanmethanol Moiety of Methanofuran. *Biochemistry* **53**:4635-4647.
- 429 11. **Wang Y, Jones MK, Xu H, Ray WK, White RH.** 2015. Mechanism of the Enzymatic
430 Synthesis of 4-(Hydroxymethyl)-2-furancarboxaldehyde-phosphate (4-HFC-P) from
431 Glyceraldehyde-3-phosphate catalyzed by 4-HFC-P synthase. *Biochemistry* **54**:2997-
432 3008.
- 433 12. **Kezmarsky ND, Xu H, Graham DE, White RH.** 2005. Identification and
434 characterization of a L-tyrosine decarboxylase in *Methanocaldococcus jannaschii*.
435 *Biochim. Biophys. Acta* **1722**:175-182.
- 436 13. **Wang Y, Xu H, Harich KC, White RH.** 2014. Identification and Characterization of a
437 Tyramine-Glutamate Ligase (MfnD) Involved in Methanofuran Biosynthesis.
438 *Biochemistry* **53**:6220-6230.
- 439 14. **Grochowski LL, Censky K, Xu H, White RH.** 2012. A new class of adenylate kinase in
440 methanogens is related to uridylate kinase. *Archives of microbiology* **194**:141-145.
- 441 15. **Xu Z, Liu Y, Yang Y, Jiang W, Arnold E, Ding J.** 2003. Crystal structure of D-
442 Hydantoinase from *Burkholderia pickettii* at a resolution of 2.7 Angstroms: insights into
443 the molecular basis of enzyme thermostability. *J. Bacteriol* **185**:4038-4049.
- 444 16. **Lira LM, Vasilev D, Pilli RA, Wessjohann LA.** 2013. One-pot synthesis of
445 organophosphate monoesters from alcohols. *Tetrahedron. Lett.* **54**:1690-1692.
- 446 17. **Delmelle M.** 1978. Investigation of Retinal as a Source of Singlet Oxygen. *Photochem*
447 *Photobiol* **27**:731-734.
- 448 18. **Miller D, O'Brien K, Xu H, White RH.** 2014. Identification of a 5'-deoxyadenosine
449 deaminase in *Methanocaldococcus jannaschii* and its possible role in recycling the

- 450 radical S-adenosylmethionine enzyme reaction product 5'-deoxyadenosine. J. Bacteriol
451 **196**:1064-1072.
- 452 19. **Rusnak P, Haney P, Konisky J.** 1995. The adenylate kinases from a mesophilic and
453 three thermophilic methanogenic members of the Archaea. J. Bacteriol. **177**:2977-29781.
- 454 20. **Ferber DM, Haney PJ, Berk H, Lynn D, Konisky J.** 1997. The adenylate kinase genes
455 of *M. voltae*, *M. thermolithotrophicus*, *M. jannaschii*, and *M. igneus* define a new family
456 of adenylate kinases. Gene **185**:239-244.
- 457 21. **Bult CJ, White O, Olsen GJ, Zhou L, Fleischmann RD, Sutton GG, Blake JA,**
458 **FitzGerald LM, Clayton RA, Gocayne JD, Kerlavage AR, Dougherty BA, Tomb JF,**
459 **Adams MD, Reich CI, Overbeek R, Kirkness EF, Weinstock KG, Merrick JM,**
460 **Glodek A, Scott JL, Geoghagen NS, Venter JC.** 1996. Complete genome sequence of
461 the methanogenic archaeon, *Methanococcus jannaschii*. Science **273**:1058-1073.
- 462 22. **Hanson AD, Gregory JF, 3rd.** 2011. Folate biosynthesis, turnover, and transport in
463 plants. Annu. Rev. Plant. Biol. **62**:105-125.
- 464 23. **Jurgenson CT, Begley TP, Ealick SE.** 2009. The structural and biochemical
465 foundations of thiamin biosynthesis. Annu. Rev. Biochem. **78**:569-603.
- 466 24. **Tarshis LC, Proteau PJ, Kellogg BA, Sacchettini JC, Poulter CD.** 1996. Regulation
467 of product chain length by isoprenyl diphosphate synthases. Proc Natl Acad Sci USA
468 **93**:15018-15023.
- 469 25. **Starks CM, Back K, Chappell J, Noel JP.** 1997. Structural basis for cyclic terpene
470 biosynthesis by tobacco 5-epi-aristolochene synthase. Science **277**:1815-1820.

- 471 26. **Lesburg CA, Zhai G, Cane DE, Christianson DW.** 1997. Crystal structure of
472 pentalenene synthase: mechanistic insights on terpenoid cyclization reactions in biology.
473 *Science* **277**:1820-1824.
- 474 27. **Jia B, Cheong GW, Zhang S.** 2013. Multifunctional enzymes in archaea: promiscuity
475 and moonlight. *Extremophiles* **17**:193-203.
- 476 28. **Wang Y, Xu H, White RH.** 2014. beta-Alanine Biosynthesis in *Methanocaldococcus*
477 *jannaschii*. *J. Bacteriol* **196**:2869-2875.
- 478 29. **Jensen RA.** 1976. Enzyme recruitment in evolution of new function. *Annu. Rev.*
479 *Microbiol.* **30**:409-425.
- 480 30. **Koga Y, Morii H.** 2007. Biosynthesis of ether-type polar lipids in archaea and
481 evolutionary considerations. *Microbiol. Mol. Biol. Rev.* **71**:97-120.
- 482 31. **Payandeh J, Fujihashi M, Gillon W, Pai EF.** 2006. The crystal structure of (S)-3-O-
483 geranylgeranylglyceryl phosphate synthase reveals an ancient fold for an ancient enzyme.
484 *J. Biol. Chem* **281**:6070-6078.
- 485 32. **Chiu HJ, Reddick JJ, Begley TP, Ealick SE.** 1999. Crystal structure of thiamin
486 phosphate synthase from *Bacillus subtilis* at 1.25 Å resolution. *Biochemistry* **38**:6460-
487 6470.
- 488 33. **Yun MK, Wu Y, Li Z, Zhao Y, Waddell MB, Ferreira AM, Lee RE, Bashford D,**
489 **White SW.** 2012. Catalysis and sulfa drug resistance in dihydropteroate synthase.
490 *Science* **335**:1110-1114.
- 491 34. **Hampele IC, D'Arcy A, Dale GE, Kostrewa D, Nielsen J, Oefner C, Page MG,**
492 **Schonfeld HJ, Stuber D, Then RL.** 1997. Structure and function of the dihydropteroate
493 synthase from *Staphylococcus aureus*. *J. Mol. Biol* **268**:21-30.

- 494 35. **Peapus DH, Chiu HJ, Campobasso N, Reddick JJ, Begley TP, Ealick SE.** 2001.
495 Structural characterization of the enzyme-substrate, enzyme- intermediate, and enzyme-
496 product complexes of thiamin phosphate synthase. *Biochemistry* **40**:10103-10114.
497
498
499
500
501
502
503
504
505
506
507

508
509
510
511
512

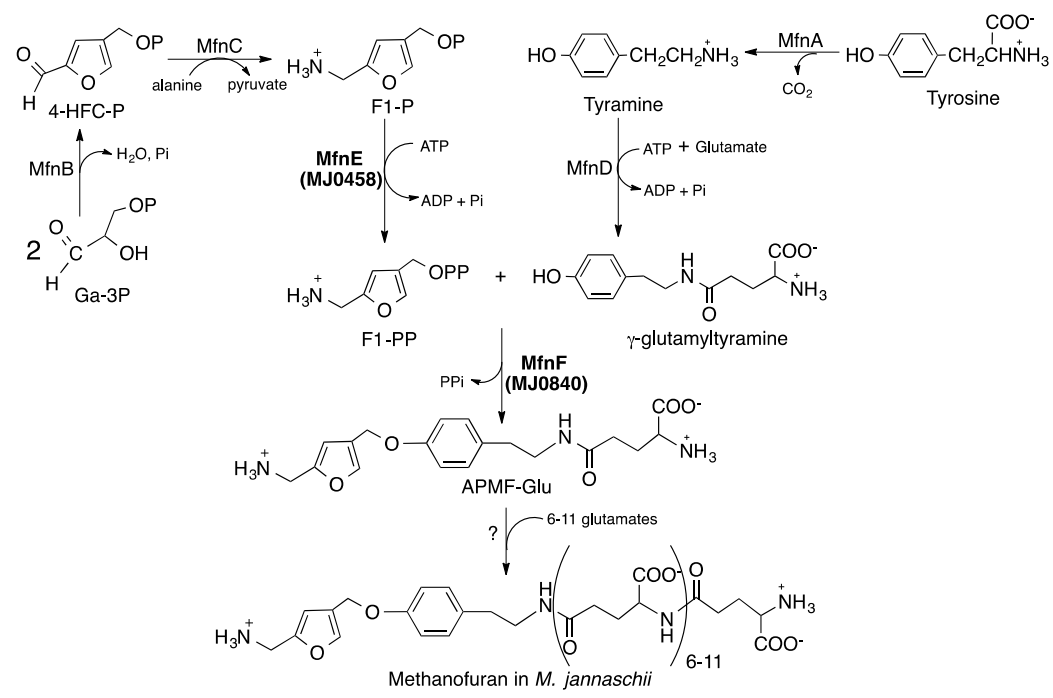
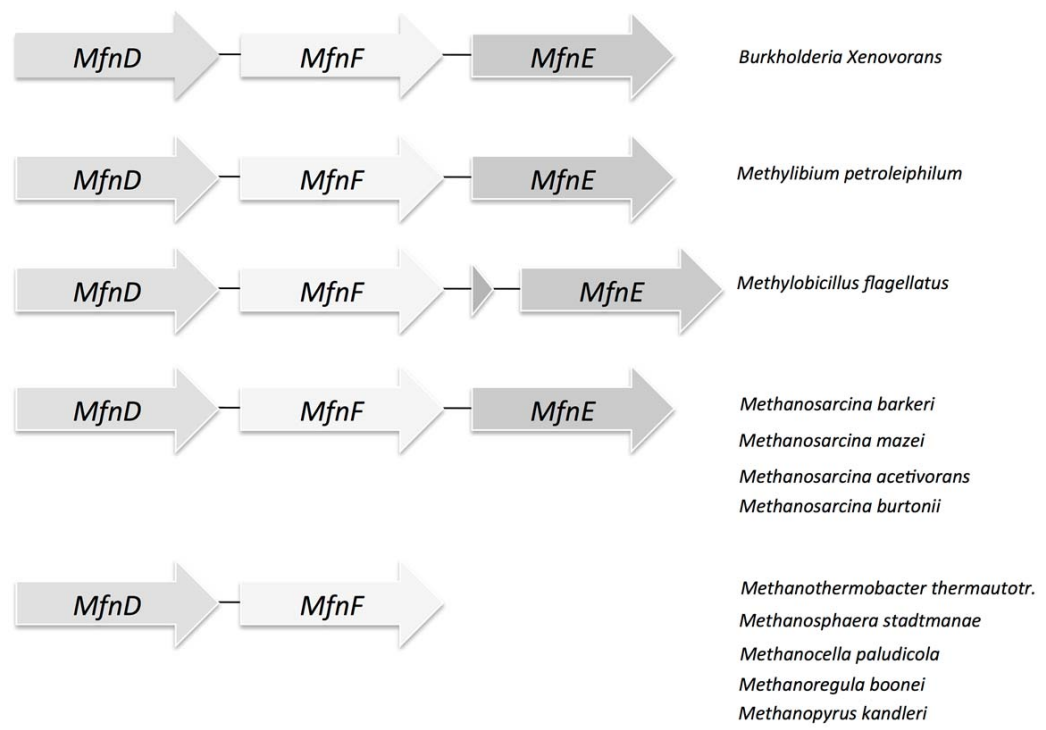


FIG 1 The proposed biosynthetic pathway of methanofuran in *M. jannaschii*.



513

514 **FIG 2** Clustering of *MfnE* (*mj0458*) and *MfnF* (*mj0840*) genes with the methanofuran
515 biosynthetic related gene *MfnD* (*mj0815*) in some methanogen and methylotroph genomes.

516

517

518

519

520

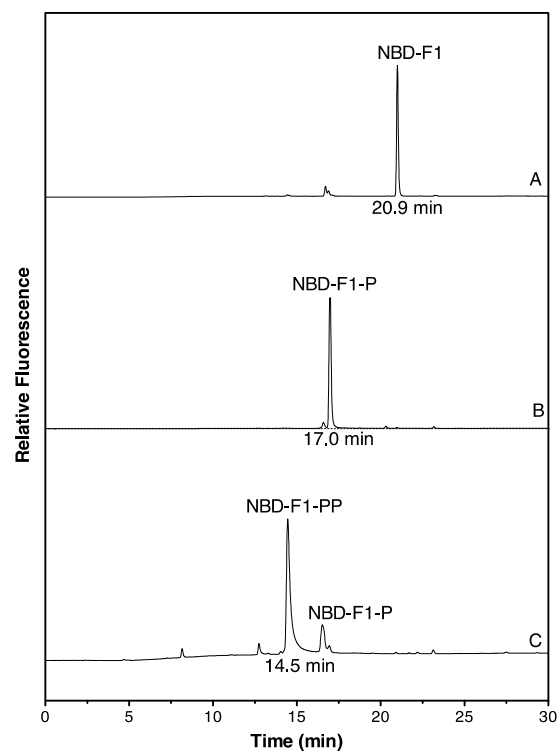
521

522

523

524

525

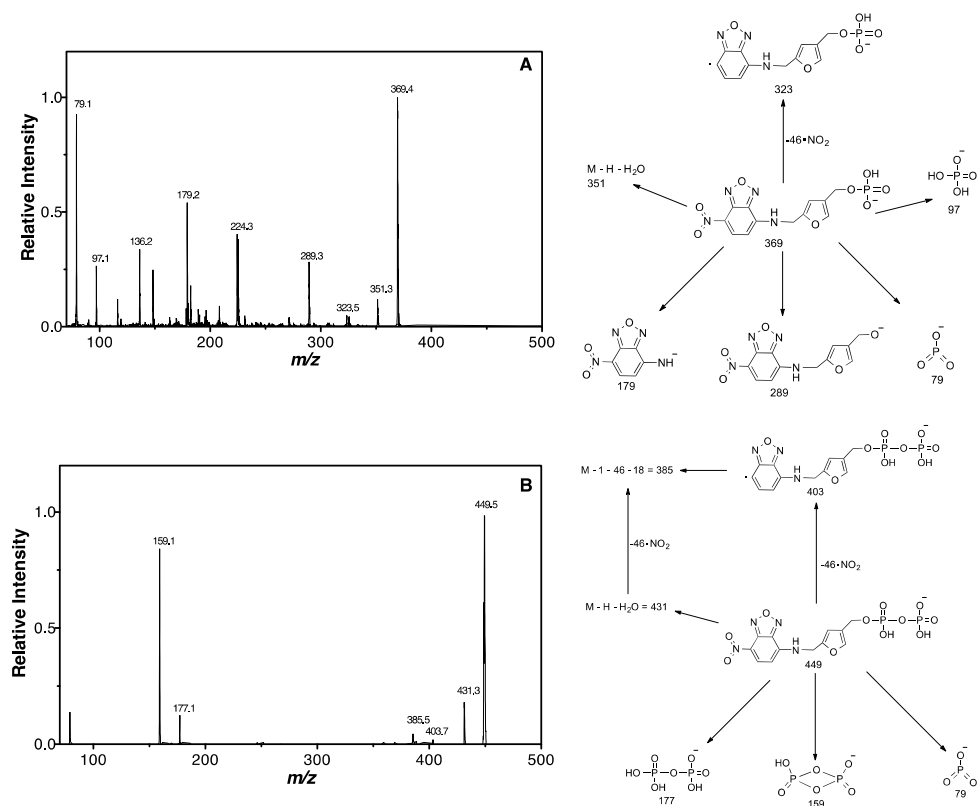


526

FIG 3 HPLC analysis of NBD-F1, NBD-F1-P, and NBD-F1-PP. A) 80 μ M sample of synthetic F1-P was converted to NBD-F1-P treated with phosphatase (37°C, 20 min) to produce NBD-F1 to confirm the structure of F1-P; B) the NBD derivatives of a reaction mixture including 80 μ M F1-P and 500 μ M ATP in the absence of MfnE (70°C, 60 min); C) the NBD derivative of a reaction mixture containing 80 μ M F1-P and 500 μ M ATP in the presence of 3.7 μ M MfnE (70°C, 60 min). Reactions in B and C are carried out in 50 mM TES buffer in the presence of 5 mM Mg^{2+} and 5 mM K^{+} at pH 7.0. The NBD derivatives were detected by fluorescence using an excitation wavelength of 480 nm and an emission wavelength of 542 nm.

535

536



537

538 **FIG 4 A)** The MS/MS spectrum of NBD-F1-P (M-H^-) = 369.4 m/z ion with the expected

539 fragments at 79, 97, 179, 289, and 323 m/z . The proposed structures of the expected fragments

540 are shown on the right. B) The MS/MS spectrum of NBD-F1-PP (M-H^-) = 449.5 m/z ion

541 generated from the phosphoryl transfer reaction between ATP and F1-P catalyzed by MfnE with

542 the expected fragments at 79, 159, 177, and 403 m/z . The proposed structures of the expected

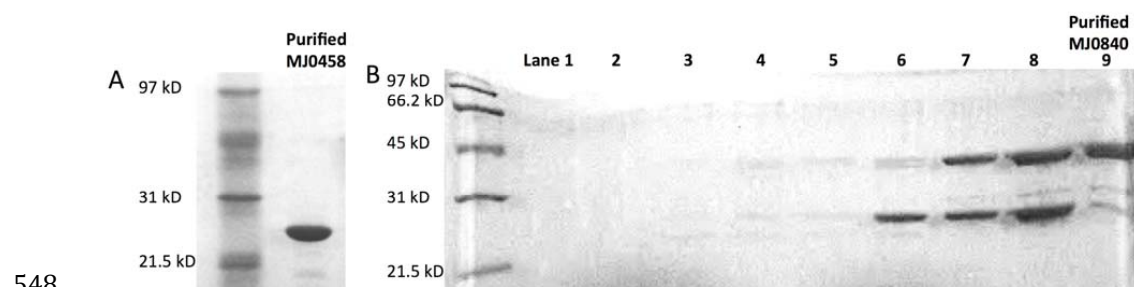
543 fragment are shown on the right.

544

545

546

547



548

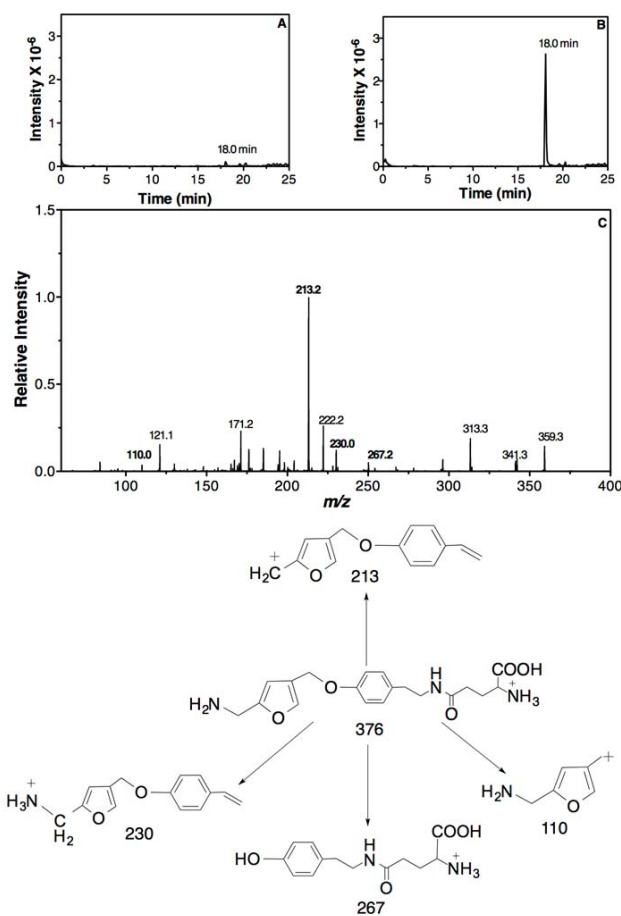
549 **FIG 5** Purification of the *mj0458* gene product (A) and *mj0840* gene product (B). In panel B,

550 lane 7 - 9 represents the target protein in the fractions eluting at 350 - 460 mM NaCl from a

551 MonoQ anion exchange column. The target protein was about 90 % pure in the fraction in lane 9.

552

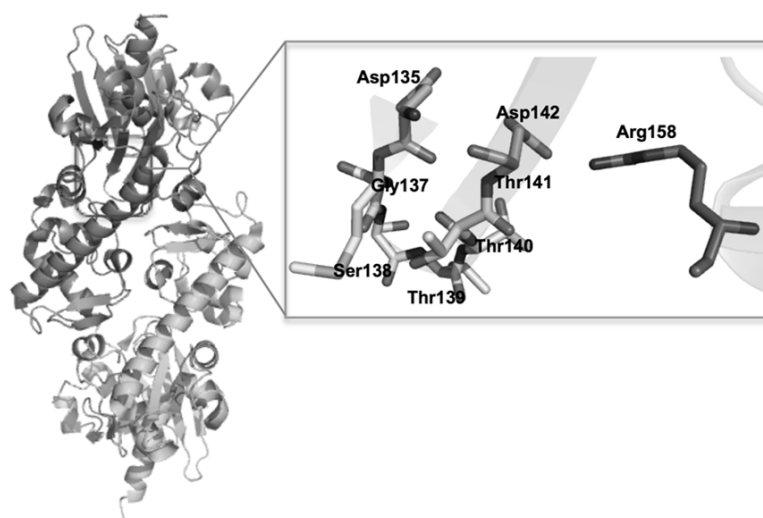
553



554

555 **FIG 6** LC/MS/MS analysis of APMF-Glu in the positive ion mode. The extracted ion
556 chromatograph (XIC) of $MH^+ = 376.2$ m/z ion from the control experiment (A) (incubate F1-P
557 with γ -glutamyltyramine in presence of MfnF) and (B) from the reaction mixture of MfnF
558 containing F1-PP generated from the MfnE reaction and γ -glutamyltyramine. (C) The MS/MS
559 spectrum of $MH^+ = 376.2$ m/z ion with the expected fragments at 110, 213, 230, and 267 m/z .
560 The proposed structures of observed fragments are shown in the bottom of the figure.

561



562

563 **FIG 7** The overall dimer structure of MfnF (left) and the possible pyrophosphate and metal-
564 binding pocket (right).

565

566

567

568

569

570

571

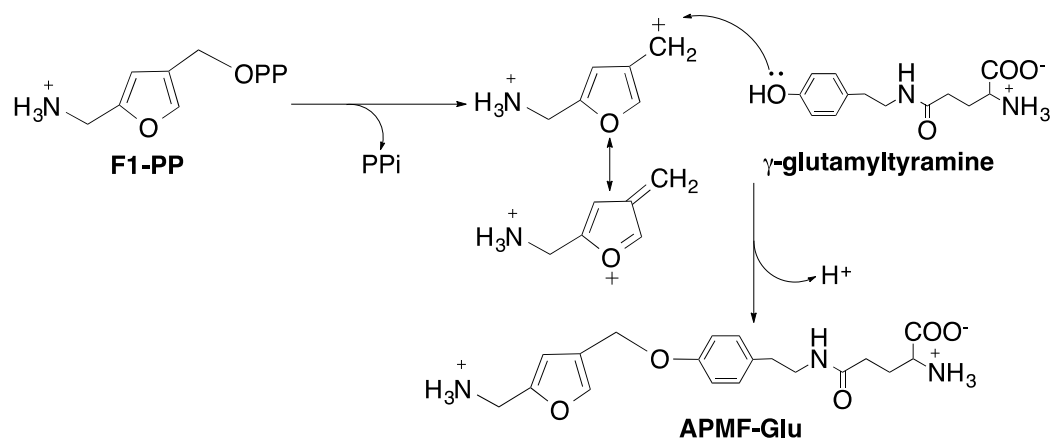


FIG 8 The proposed catalytic mechanism of MfnF.

